Differential Phase-Shift Keying in Spatial Diversity Transmitters for Fade Mitigation

Todd G. Ulmer, *Member, IEEE*, Scott R. Henion, Frederick G. Walther, *Member, IEEE*, and Peter A. Schulz, *Member, IEEE*

***Abstract*—We investigate the use of differential phase-shift keying (DPSK) in multiwavelength spatial diversity transmitters for mitigation of atmospheric fading. By selecting the transmitter wavelengths to coincide with the transmission peaks of the delay-line interferometer in the receiver, the only modification required to a standard DPSK receiver is a wider optical filter. We examine the wavelength separation required to minimize penalties from beating between the wavelengths and find that a separation of twice the data rate is sufficient for a four-wavelength system with narrow filtering. We also demonstrate a reduction in scintillation loss for a four-wavelength DPSK system in a fading channel.**

***Index Terms*—Differential phase-shift keying (DPSK), diversity methods, fading channels, optical amplifiers, optical communication, random media.**

I. Introduction

THE transmission of multiple, co-aligned, spatially diverse beams is a well-known method of mitigating scintillation from atmospheric turbulence in free-space optical links [1]–[16]. By distributing the available transmitter power across N spatially separated beams, the intensity received in the far field, where the diverging beams overlap, becomes the sum of N independent, identically distributed random variables, and the scintillation variance is reduced by a factor of N. Thus, the use of a spatial diversity transmitter is a powerful scintillation mitigation technique for links where atmospheric turbulence occurs in the far field of the receiver, e.g., uplinks from the ground and horizontal links within the atmosphere. Spatial diversity techniques can be used in conjunction with coding and interleaving to provide robust communications performance [17]; however, by actually reducing the scintillation variance, spatial diversity also alleviates requirements on clock recovery and spatial tracking systems, whereas temporal diversity techniques alone do not.

Wavelength detuning of the N lasers in a spatial diversity transmitter can be used to minimize interferometric beating at the common photodetector in the receiver. While the different lasers are not phase locked, if tuned to the same wavelength they will produce beating with a phase that varies on the time scale of the laser coherence time; this beating can result in significant power penalties. By separating the carrier frequencies by at least the bandwidth of the receiver, beating effects can be minimized. While this minimal wavelength separation does not provide any significant scintillation reduction from wavelength diversity, it does allow the minimization of the penalty from the wide optical filter required in the receiver.

Spatial diversity transmitters have been demonstrated in a variety of systems. Several commercial free-space optical systems use spatial diversity to mitigate scintillation in building-to-building links with ranges on the order of a few kilometers [10]. At the other extreme, diversity transmitters have been used in several ground-to-space demonstrations with ranges up to $\sim$40 000 km, including NASA's GOLD uplink from the ground to the Japanese ETS-VI satellite [2], [3], the European Space Agency's SILEX uplink from the ground to the Artemis satellite [8], [9], and the Japanese National Institute of Information and Communication Technology's recent uplink from the ground to the OICETS/Kirari satellite [13]. All three of these uplink demonstrations used four beams. An eight-beam diversity transmitter had been investigated for a $\sim$200 000 000-km Earth-to-Mars uplink in NASA's Mars Laser Communication Demonstration program prior to cancellation of the host mission [12].

The choice of modulation format is crucial for lasercom systems, where high-sensitivity receivers enable smaller apertures and lower transmitter powers. Because the multiple beams from a diversity transmitter are summed at a common photodetector in the receiver, modulation formats compatible with direct detection receiver architectures (such as ON-OFF keying (OOK) and pulse-position modulation (PPM)) have been used for most spatial diversity systems to date. However, differential phase-shift keying (DPSK), which requires only bit-to-bit coherence in the individual beams, is also amenable to spatial diversity transmission. DPSK is now widely recognized as an attractive modulation format for fiber-optic communication systems, where scintillation is not an issue [18]. DPSK provides a significant advantage in receiver sensitivity, reducing the required transmitter power for a given link: for an optically preamplified direct-detection receiver operating at a bit-error ratio (BER) of 10^{-9}, DPSK is fundamentally 2.8 dB more sensitive than OOK and 3.0 dB more sensitive than orthogonal modulation formats such as binary frequency-shift keying and binary PPM [19]. In addition, DPSK has been demonstrated with small implementation losses over a wide range of data rates, ensuring that the fundamental sensitivity benefits can be realized in practice [20]–[22]. A DPSK receiver can be implemented in a straightforward manner, using a one-bit delay-line interferometer

Manuscript received August 28, 2009; revised October 16, 2009; accepted November 6, 2009. Date of publication January 8, 2010; date of current version October 6, 2010. This work was supported by the Department of the Air Force under Air Force Contract FA8721-05-C-0002. Opinions, interpretations, conclusions, and recommendations are those of the authors and are not necessarily endorsed by the United States Government.

The authors are with the Advanced Lasercom Systems and Operations Group, MIT Lincoln Laboratory, Lexington, MA 02420 USA (e-mail: ulmer@ll.mit.edu; henion@ll.mit.edu; fgwalther@ll.mit.edu; pschulz@ll.mit.edu).

Color versions of one or more of the figures in this paper are available online at http://ieeexplore.ieee.org.

Digital Object Identifier 10.1109/JSTQE.2009.2036861

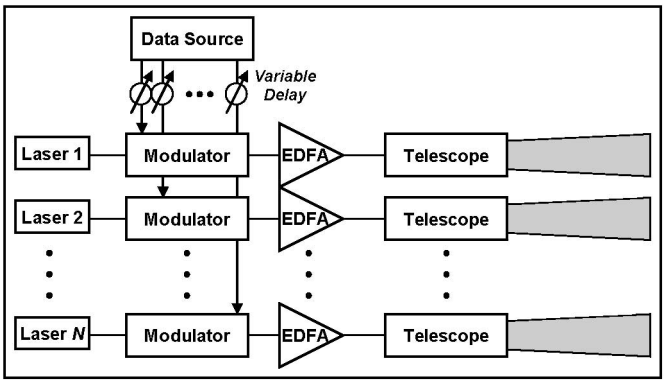

Fig. 1. Spatial diversity transmitter with master oscillator/power amplifier architecture. Each of N signal paths is modulated with identical data and connected to an individual telescope or sub-aperture of a common telescope. Path matching and variable delays are used to ensure the signals exiting the telescope(s) are synchronized. Each beam is initially separated from the others by a distance large enough that fading of the different beams is uncorrelated. The beams overlap in the far field such that all of them illuminate the receiver. EDFA: erbium-doped fiber amplifier.

as an optical demodulator combined with balanced photodetection [23]. With the proper selection of wavelengths, a common delay-line interferometer can be used to demodulate multiple wavelength-division-multiplexed channels [24], which we exploit here to enable a simple receiver for use with a spatial diversity DPSK transmitter.

Here, we investigate the use of DPSK modulation with a 10.7-Gb/s spatial diversity transmitter. We select the N transmitter wavelengths to be separated by a multiple of the line rate so that a single delay-line interferometer can be used to demodulate them for detection with a common balanced photodetector pair. We assess the details of implementation, including the required wavelength accuracy and stability of the transmitter and minimum wavelength spacing to avoid beating effects. For a four-beam system with an electrical bandwidth of $\sim$1.2 times the line rate, we find that a wavelength separation of twice the line rate produces measurable beating effects, while a separation of three times the line rate is sufficient to render the beating penalty negligible. However, we find that narrow optical filtering can allow similar performance to be achieved for both cases. We also demonstrate a four-wavelength system in the presence of a fading channel, showing the benefit of DPSK diversity by comparison to single-wavelength results in the same channel.

II. Implementation

An example of a spatial diversity transmitter is shown schematically in Fig. 1. To transmit information, multiple beams are imparted with identical data modulation and launched through individual telescopes or subapertures of a common telescope. The path lengths from the data modulators to the apertures must be matched to within a small fraction of a bit period to synchronize the bits across different beams. The multiple apertures are physically separated by a large distance so that each beam experiences independent turbulence conditions as it propagates through the atmosphere. Thus, the beams produce different time-varying spatial profiles that overlap in the far field, each resulting in a unique scintillation pattern at the receiver aperture. The receiver optics couple the beams onto a common photodetector, and the penalty associated with the deep fade of any one beam is minimized because the power fades of the different beams are uncorrelated. The probability of a deep fade with multiple beams is the joint probability of simultaneous deep fades on all beams, an event with a dramatically lower probability than a fade on a single beam. We note that significant fade mitigation can still be obtained even if the beams are not completely uncorrelated [15]. Furthermore, a spatial diversity transmitter only mitigates turbulence that occurs in the far field of the receiver, i.e., near the transmitter; thus, in a horizontal link, the phase distortion caused by turbulence near the receiver may require additional mitigation from, e.g., spatial diversity receivers [25]–[30] or adaptive optics.

A high-rate lasercom system employing a spatial diversity transmitter trades robustness to fading for additional complexity at the transmitter and a power penalty from the wide optical filter required in the receiver [16]. N copies of the transmitter hardware are needed, along with path matching at the symbol level, which may be achieved through optical or microwave delay lines. However, because the normalized standard deviation of the intensity delivered to the receiver scales as $1/\sqrt{N}$ [1], the largest reduction in overall dynamic range occurs with the first set of duplicate hardware ($N = 2$), with diminishing additional benefit for each successive transmitter path. Thus, most commercial systems and space demonstrations have been accomplished using only two to four beams. To avoid interferometric beating between the beams at the square-law photodetectors in the receiver, the carrier frequencies of the individual beams must be separated by more than the electrical bandwidth of the receiver. As a result, the optical filter in the receiver must be sufficiently broad to pass all N wavelengths, incurring a power penalty relative to a single-wavelength receiver. In an optically preamplified receiver, the wide optical filter transmits excess amplified spontaneous emission (ASE) as well as excess optical background noise.

The benefits of a spatial diversity transmitter can be achieved with minimal modification to a single-wavelength DPSK receiver design; the primary change is the wider optical filter to accommodate the multiple wavelengths. A DPSK demodulator is typically implemented using a one-bit delay-line interferometer, which has a periodic frequency response with transmission peaks separated by the line rate of the framed data stream (e.g., 10.7 GHz for Optical Transport Unit 2). Thus, multiple beams can be demodulated with a single interferometer, so long as their wavelengths are selected to correspond the transmission peaks of the interferometer.

At the transmitter, spatially diverse DPSK requires accurate control of the multiple wavelengths and *a priori* knowledge of the DPSK demodulator. Whereas with spatial diversity PPM or OOK the wavelength spacing can vary continuously, with DPSK the wavelength spacing must be precisely matched to a multiple of the interferometer free spectral range (FSR). The sensitivity to frequency mismatch has been analyzed and reported in the literature in the context of WDM demultiplexing [24], [31]; a frequency mismatch of $\sim\pm$3% of the interferometer

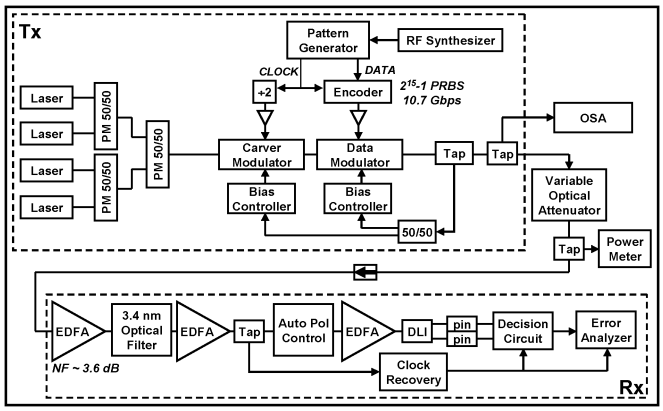

Fig. 2. Four-wavelength diversity transmitter configuration for wavelength spacing experiments. PM: Polarization maintaining; RF: radio frequency; PRBS: pseudo-random bit sequence; OSA: optical spectrum analyzer; EDFA: erbium-doped fiber amplifier; NF: noise figure; DLI: delay-line interferometer; pin: pin photodiode.

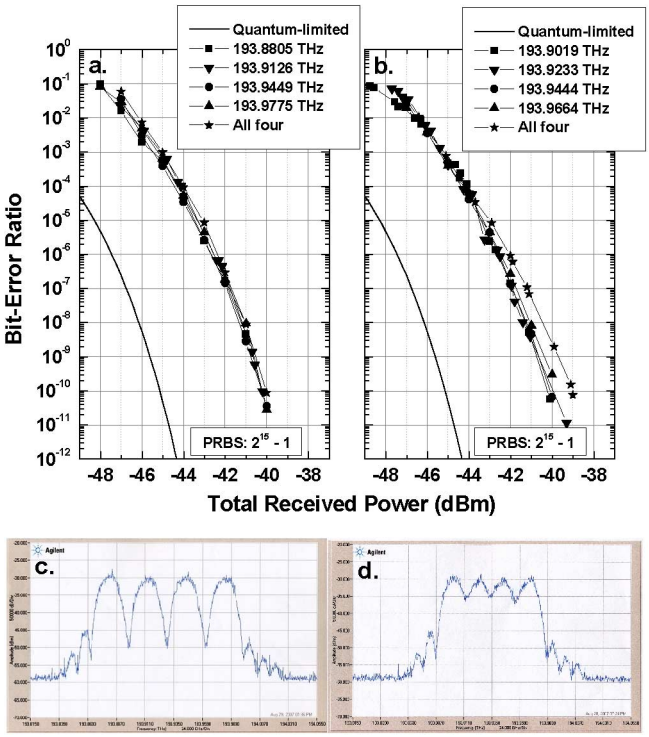

Fig. 3. BER results and transmitter optical spectra for four-wavelength diversity transmitter with wavelengths spaced by three free spectral ranges (FSRs) ((a) and (c)) and two FSRs((b) and (d)). Beating effects are negligible with all four wavelengths present for the three FSR spacing, while a 0.9 dB beating penalty at BER $= 10^{-9}$ is present for the two FSR spacing. PRBS: pseudo-random bit sequence.

FSR will contain the penalty to $<$1.0 dB. For a 10-Gb/s signal in the 1550-nm band, this corresponds to a wavelength accuracy of $\pm$2.4 pm, which is readily achievable using commercial laser sources with precise temperature control. For InP lasers near 1550 nm, the emission wavelength can be temperature tuned by $\sim$100 pm/K [32]; temperature control with stability of 10 mK is therefore sufficient [33]. Slow closed-loop control of the laser and interferometer wavelengths would be required in a fielded system; however, for the laboratory experiments described below no such control was needed.

III. Experiments

A. Wavelength Spacing

The four-wavelength, 10.7-GHz return-to-zero (RZ) system shown in Fig. 2 was used to demonstrate the demodulation and detection of multiple DPSK beams using a common interferometer and balanced photodetector pair and to explore the required laser wavelength spacing [34]. The transmitter consisted of four tunable external cavity lasers combined with polarization-maintaining 3-dB couplers and modulated with a 10.7-GHz 2^{15}-1 pseudo-random bit sequence (PRBS) via lithium niobate carver and data modulators. The optically preamplified receiver incorporated a 430-GHz (3.4-nm) filter after the first optical amplifier to accommodate multiwavelength operation. An active polarization controller was used with a polarizer to filter ASE $\times$ ASE noise in the polarization orthogonal to the signal. The electrical bandwidth of the receiver was set by the photodetectors, which have a 3-dB frequency of $\sim$12.8 GHz, and the decision circuit was a 50-GHz D flip-flop. Tuning of the interferometer in the receiver was accomplished thermally by locking to an out-of-band pilot-tone laser. The individual transmit lasers were tuned to match the desired transmission peak of the interferometer using a wave meter and then optimized individually by fine-tuning the wavelength to minimize the BER. At a BER 10^{-4}, the same receiver operates 2.3 dB from the quantum limit for preamplified DPSK using an 18-GHz optical filter with a single wavelength at 10.7 Gb/s. The wider filter for diversity operation resulted in $\sim$2.8 dB of additional implementation penalty, shifting the single-wavelength 10^{-4} BER receiver sensitivity to 5.1 dB from quantum-limited.

Two different cases were investigated, one where the four wavelengths were each separated by three interferometer FSRs ($\sim$32 GHz) and one where the four wavelengths were separated by two FSRs ($\sim$21 GHz). The wavelengths were centered on $\sim$1545.9 nm, and the four modulated carriers were of equal power to within $\pm$0.5 dB. The BER results from the three-FSR case are shown in Fig. 3(a), where the theoretical result for a quantum-limited optically preamplified DPSK receiver is shown for reference [19]. Nearly identical performance is achieved with each of the individual signals as well as all four together, confirming the absence of significant beating effects.

In contrast, beating effects are present when the carriers are separated by only two interferometer FSRs (see Fig. 3(b)). In this case, all the BER curves for the individual wavelengths are similar in performance, but the ensemble is degraded by 0.9 dB at BER $= 10^{-9}$. We attribute the degraded performance to the beating between adjacent signals that falls within the receiver electrical bandwidth. The effect is most pronounced at low BER, i.e., where the signal is strong.

The presence of a beating penalty was confirmed using a different experimental setup, shown in Fig. 4. Two significant differences in the receiver were the incorporation of a variable-bandwidth tunable optical filter and the absence of a polarization

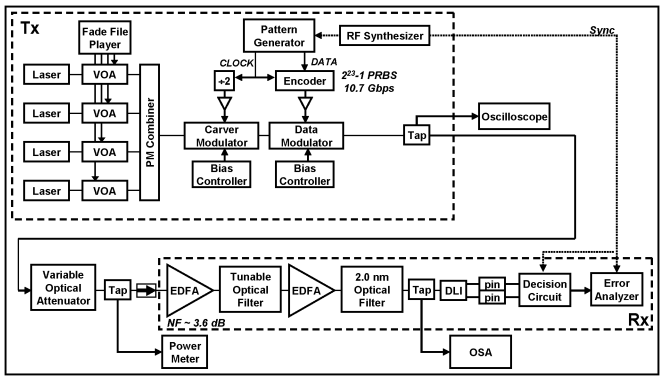

Fig. 4. Four-wavelength diversity transmitter configuration for wavelength spacing and fading channel experiments. VOA: variable optical attenuator; PM: polarization maintaining; RF: radio frequency; PRBS: pseudo-random bit sequence; EDFA: erbium-doped fiber amplifier; NF: noise figure; OSA: optical spectrum analyzer; DLI: delay-line interferometer; pin: pin photodiode.

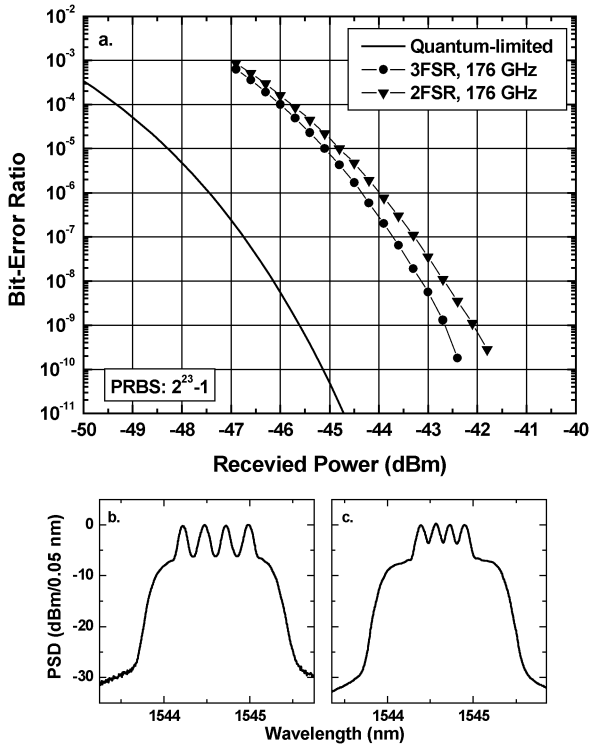

Fig. 5. (a) BER measurements and corresponding optical spectra prior to the delay-line interferometer with a 176-GHz (1.4-nm) optical filter for: (b) three-FSR wavelength spacing and (c) two-FSR spacing. Beating between wavelengths is evident for the two-FSR case, particularly, at low BER. PRBS: pseudo-random bit sequence; PSD: power spectral density.

filter. The variable optical attenuators (VOAs) in the transmitter were not used for the results in this section and are described in Section III-B. Once again, wavelength spacings of three and two FSRs were investigated using four wavelengths modulated by a common carver/data modulator pair. The results are shown in Fig. 5, where a 2^{23}-1 PRBS was used. The wavelengths were centered on $\sim$1544.6 nm, and the four wavelengths were of equal power within $\pm$0.2 dB. The electrical bandwidth of the

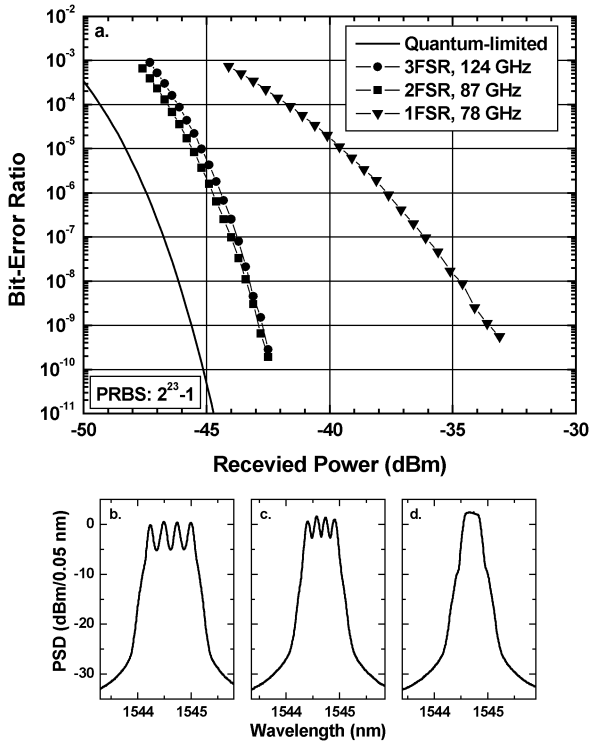

Fig. 6. (a) BER measurements and corresponding optical spectra prior to the delay-line interferometer with optimized optical filtering for: (b) three-FSR wavelength spacing, (c) two-FSR spacing, and (d) one-FSR wavelength spacing (peaks not resolved by spectrum analyzer). Beating between wavelengths is significant for the one-FSR case. PRBS: pseudo-random bit sequence; PSD: power spectral density.

receiver was again set by the $\sim$12.8-GHz photodetectors, and the decision circuit was a 25-GHz latched comparator. Results are shown for an optical filter bandwidth of 176 GHz (1.4 nm), which is sufficiently wide to pass all four wavelengths without clipping for the three-FSR case. A beating penalty of 0.3 dB at BER $= 10^{-4}$ and 0.6 dB at BER $= 10^{-9}$ was observed.

Despite the presence of beating, wavelength separation of two FSRs can achieve similar sensitivity to the three-FSR case if narrow optical filtering is used. In Fig. 6, four-wavelength results are shown for three-, two-, and one-FSR cases where the optical filter bandwidth has been set to obtain the optimum balance between excess ASE noise and clipping of the two outside wavelengths at a BER of $\sim 10^{-6}$. In each case, the optimum filter setting was found by holding the input power constant and varying the filter bandwidth while monitoring the BER. The experimentally determined optimum filter bandwidths were found to be 124 , 87 , and 78 GHz for three-, two-, and one-FSR spacing, respectively. We note that the insertion loss of our tunable filter begins to increase for narrow bandwidths, and thus a lower loss filter might result in a narrower optimum bandwidth for the one-FSR case. Fig. 6 shows that the two-FSR case can achieve similar or slightly better sensitivity than the three-FSR case; with optimized optical filtering, the beating penalty for the two-FSR case is compensated by the reduced ASE noise with the narrower filter. We note that beating might be somewhat reduced with this narrow filtering, as the outer wavelengths are slightly

clipped by the filter. In a fading channel, a slightly wider filter might be necessary to achieve the full benefit of the diversity transmitter.

Given that the 3-dB electrical bandwidth of our receiver exceeds one FSR, significant beating effects are expected for the one-FSR wavelength spacing. As shown in Fig. 6, this was indeed observed experimentally. The one-FSR case exhibits a strong beating penalty, indicating that the beating dominates over the ASE noise. We note that our receivers have excess electronic bandwidth (∼13-GHz photodetectors supporting 10.7-Gb/s data), and thus beating might be reduced with additional electrical filtering.

Two- and three-wavelength cases with various wavelength separations were also investigated with both experimental setups; the beating penalty was found to be small but measurable with wavelength spacings of two interferometer FSRs and negligible for separation of three FSRs, which is consistent with the four-wavelength results.

Polarization interleaving might be used to improve the receiver sensitivity by allowing a more compact spectrum, with the potential for tighter filtering and improved ASE rejection [16]. This can be achieved by polarization interleaving the wavelengths at the transmitter such that the closest two co-polarized wavelengths are sufficiently separated to avoid beating within the receiver electronic bandwidth. A polarization-independent receiver would be needed to support this mode of operation. Furthermore, a periodic filter matched to the grid of the incoming wavelengths combined with a pass-band filter matched to the total wavelength span could be used to reduce excess optical noise, optimizing receiver sensitivity.

B. Fading Channel

The RZ-DPSK system in Fig. 4 was used to verify the performance of diversity DPSK in a fading channel. To emulate atmospheric fading, high-speed VOAs with closed-loop control were inserted into each of the four transmitter paths. Each VOA was driven with a time series generated by wave-optics simulation of a 26.6-km uplink from the ground to an aircraft traveling at 75 kn (38.6 m/s). The link simulation was configured for an 11-mm transmit aperture, a Hufnagel-Valley 5/7 atmosphere [35], and an elevation angle of 20°, corresponding to an aircraft altitude of 30 000 ft. The simulation assumed atmospheric tilt is corrected on the uplink beam by a fast steering mirror in the ground terminal with a 1-kHz tracking loop using the downlink beam from the aircraft as a reference. Fig. 7 shows the simulated time series, and Fig. 8 shows its probability density function and cumulative distribution function. The VOA closed-loop bandwidth is ∼400 Hz, which is more than sufficient to provide a realistic approximation of the simulated atmospheric channel (see Fig. 9). The 15-s time series was looped on a computer and played back through D/A converters. The drive signal for each VOA incorporated a different time delay so that the individual beams would be uncorrelated but have the same fade statistics. The four wavelengths were centered on ∼1545.0 nm (Table I) and were modulated with a common carver/data modulator pair, ensuring synchronization. The optically preamplified

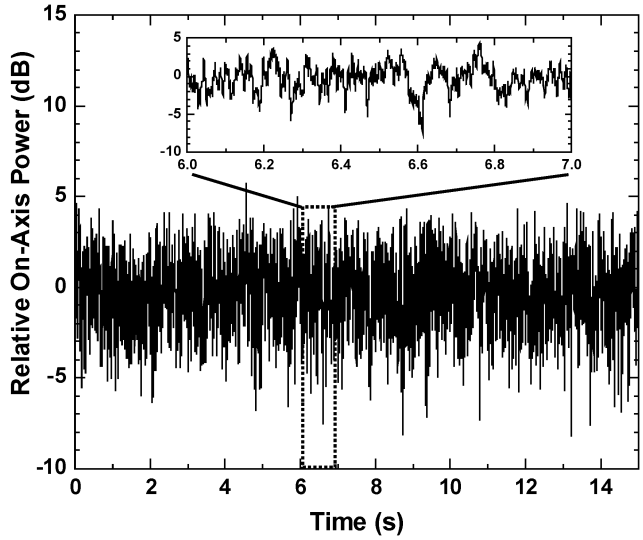

Fig. 7. Fading time series used for the experiments, representing relative on-axis power delivered to the receiver for the uplink. Detail of the time series from 6.0 to 7.0 s (inset).

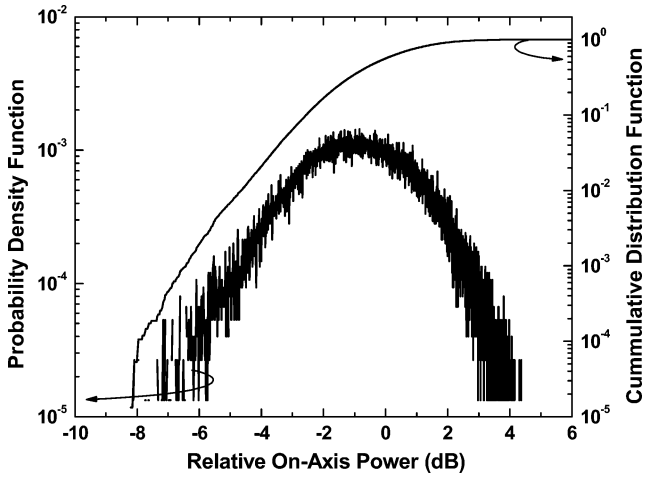

Fig. 8. Probability density function and cumulative distribution function of the fading time series.

receiver had a first stage noise figure of ∼3.6 dB and a 124-GHz (1.0 nm) optical filter without polarization filtering. The filter was set slightly wider than the optimum bandwidth found for the static channel to ensure that the outer wavelengths would not be clipped. To isolate the communications aspects of fading, direct synchronization of the pattern generator and the error detector was used rather than recovering the clock from the received optical signal.

BER results for several different conditions are shown in Fig. 10. First, data were collected without fading to establish a reference. A single-wavelength curve was recorded as a baseline, and then a four-wavelength curve was recorded with wavelength separations of two FSRs (∼21 GHz). A beating penalty of 0.6 dB was observed at a BER of 10^{-9}, consistent with the results in Fig. 5. When fading was introduced, the gate time on the BER analyzer was increased to average over the entire fading time sequence. With fading, the single wavelength

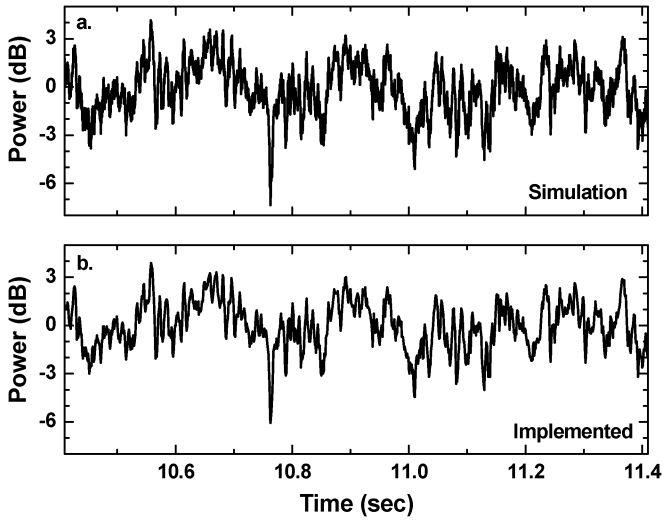

Fig. 9. (a) One-second segment of the simulated time series of relative power delivered to the receiver aperture through the fading channel for a single beam. (b) Same segment of the fading time series as implemented with a VOA with a closed-loop bandwidth of ∼400 Hz.

TABLE I
CARRIER FREQUENCIES FOR FADING CHANNEL EXPERIMENTS

Condition	Carrier Frequencies (THz)
One beam	194.0321
Four beams	194.0107
	194.0321
	194.0535
	194.0747

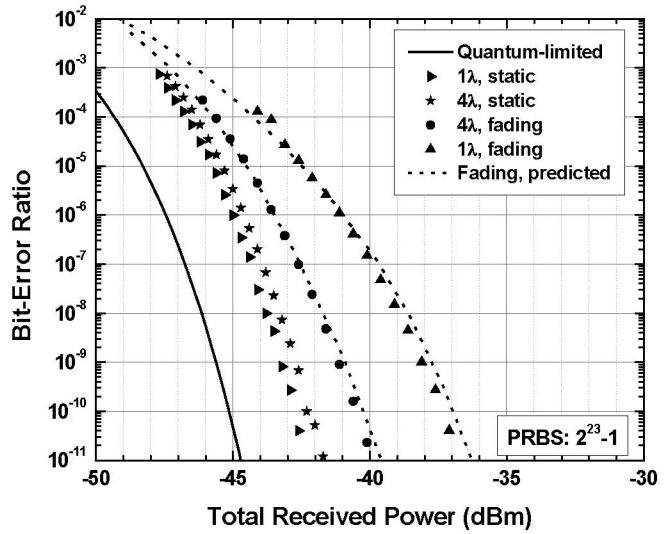

Fig. 10. BER results for single- and four-wavelength cases with and without fading for a wavelength spacing of two FSRs. The receiver optical filter bandwidth is 124 GHz, the EDFA noise figure is ∼3.6 dB, and the receiver does not incorporate a polarization filter. Predictions for the fading channel include the measured implementation losses of 2.9 dB and 2.3 dB for the four-wavelength and single-wavelength cases, respectively. PRBS: pseudo-random bit sequence.

curve was shifted by 5.2 dB (at BER $= 10^{-9}$) relative to the single-channel baseline, while the four-wavelength curve was only shifted by 1.5 dB relative to the four-wavelength baseline. Thus, even with the residual beating penalty, the receiver sensitivity for this particular fading channel is improved by a net 3.1 dB by using a four-beam system with wavelengths spaced by two FSRs. Larger reductions in scintillation loss are expected in channels with more aggressive fading.

Theoretical predictions for the fading performance are also shown in Fig. 10. These are obtained by calculating the instantaneous quantum-limited BER for each 200-μs time increment of the fading time series and then averaging over the entire 15-s time series. The process is repeated for various values of mean power delivered to the receiver to produce a plot of quantum-limited BER versus received average power in the fading channel. The curves are then shifted by the measured implementation loss (at 10^{-9}) in the static channel (2.3 dB for the single-wavelength case and 2.9 dB for the four-wavelength case, which includes the 0.6-dB beating penalty). While the assumption that the implementation loss is independent of the operating point is an approximation, the resulting agreement with the measured data is excellent, confirming that if clock recovery is reliable, the BER is determined strictly by the instantaneous power delivered to the receiver.

IV. CONCLUSION

We have shown that DPSK is compatible with the spatial diversity transmitter approach to scintillation mitigation. DPSK has a clear sensitivity advantage over the OOK and binary PPM formats often used in lasercom systems. Multiple DPSK beams can be demodulated by a common interferometer and photodetector pair with minimal penalty as long as the wavelengths are sufficiently separated to avoid beating effects within the bandwidth of the square-law photoreceiver. The primary constraint associated with spatial diversity DPSK is that the transmitter wavelengths must be tightly controlled to match the transmission peaks of the interferometer, but the level of control needed is readily achievable with commercially available hardware. We have demonstrated that wavelength separation of three times the line rate is sufficient for operation without significant beating effects in a four-wavelength system with an electrical bandwidth of ∼1.2 times the line rate, and wavelength separation of twice the line rate can also give good performance with narrow filtering. For the particular ground-to-air uplink considered here, we observe average scintillation losses of 5.2 dB for the single-wavelength case, and a net improvement of 3.1 dB with the power distributed among four beams with wavelength spacing of twice the line rate, demonstrating the efficacy of spatial diversity transmitters.

ACKNOWLEDGMENT

The authors would like to thank several of their colleagues at MIT Lincoln Laboratory for their contributions to the experiments: S. Michael for providing the atmospheric simulation, R. J. Murphy for designing and building the closed-loop control circuits for the high-speed VOAs, R. J. Magliocco for designing and building the microwave subsystems, and J. D. Moores and R. R. Parenti for useful discussions.

REFERENCES

[1] W. M. Bruno, R. Mangual, and R. F. Zampolin, "Diode laser spatial diversity transmitter," *Proc. SPIE*, vol. 1044, pp. 187–194, 1989.

[2] K. E. Wilson, J. R. Lesh, K. Araki, and Y. Arimoto, "Overview of the ground-to-orbit lasercom demonstration," *Proc. SPIE*, vol. 2990, pp. 23–30, 1997.

[3] M. Jeganathan, M. Toyoshima, K. Wilson, J. James, G. Xu, and J. Lesh, "Data analysis results from the GOLD experiments," *Proc. SPIE*, vol. 2990, pp. 70–81, 1997.

[4] I. I. Kim, H. Hakakha, P. Adhikari, E. Korevaar, and A. K. Majumdar, "Scintillation reduction using multiple transmitters," *Proc. SPIE*, vol. 2990, pp. 102–113, 1997.

[5] E. Korevaar, "Multiple transmitter laser link," U.S. Patent 5 777 768, Jul. 7, 1998.

[6] C. Higgs, H. T. Barclay, D. V. Murphy, and C. A. Primmerman, "Atmospheric compensation and tracking using active illumination," *Lincoln Lab. J.*, vol. 11, no. 1, pp. 5–26, Nov. 1, 1998.

[7] A. Biswas and S. Lee. (2000, May 15). "Ground-to-ground optical communications demonstration," NASA Jet Propulsion Lab., Pasadena, CA, TMO Progress Rep. 42-14. [Online]. Available: http://opticalcomm.jpl.nasa.gov/PAPERS/GG/141g.pdf

[8] M. Reyes, Z. Sodnik, P. Lopez, A. Alonso, T. Viera, and G. Oppenhauser, "Preliminary results of the in-orbit test of ARTEMIS with the Optical Ground Station," *Proc. SPIE*, vol. 4635, pp. 38–49, 2002.

[9] M. Reyes, S. Chueca, A. Alonso, T. Viera, and Z. Sodnik, "Analysis of the preliminary optical links between ARTEMIS and the Optical Ground Station," *Proc. SPIE*, vol. 4821, pp. 33–43, 2002.

[10] S. Bloom, E. Korevaar, J. Schuster, and H. Willebrand, "Understanding the performance of free-space optics," *J. Opt. Netw.*, vol. 2, no. 6, pp. 178–200, Jun. 2003.

[11] V. W. S. Chan, "Optical satellite networks," *J. Lightw. Technol.*, vol. 21, no. 11, pp. 2811–2827, Nov. 2003.

[12] A. Biswas, M. W. Wright, J. Kovalic, and S. Piazzolla, "Uplink beacon laser for Mars Lasercom Demonstration (MLCD)," *Proc. SPIE*, vol. 5712, pp. 93–100, 2005.

[13] M. Toyoshima, Y. Takayama, T. Takahashi, K. Suzuli, S. Kimura, K. Takizawa, T. Kuri, W. Klaus, M. Toyoda, H. Kunimori, T. Jono, and K. Arai, "Ground-to-satellite laser communication experiments," *IEEE Aerosp. Electron. Syst. Mag.*, vol. 23, no. 8, pp. 10–18, Aug. 2008.

[14] H. Hemmati, Ed., *Deep Space Optical Communications*. Hoboken, NJ: Wiley, 2006, pp. 111–112, 203, 486–488.

[15] J. A. Anguita, M. A. Neifeld, and B. V. Vasic, "Spatial correlation and irradiance statistics in a multiple-beam terrestrial free-space optical communication link," *Appl. Opt.*, vol. 46, no. 26, pp. 6561–6571, Sep. 10, 2007.

[16] T. G. Ulmer, S. R. Henion, and F. G. Walther, "Power penalty from amplified spontaneous emission in spatial diversity links for fade mitigation," *IEEE Photon. Technol. Lett.*, vol. 21, no. 3, pp. 170–172, Feb. 2009.

[17] J. A. Greco, "Design of the high-speed framing, FEC, and interleaving hardware used in a 5.4-km free-space optical communication experiment," *Proc. SPIE*, vol. 7464, pp. 746409-1–746409-7, 2009.

[18] A. H. Gnauck and P. J. Winzer, "Optical phase-shift-keyed transmission," *J. Lightw. Technol.*, vol. 23, no. 1, pp. 115–130, Jan. 2005.

[19] S. B. Alexander, *Optical Communication Receiver Design*. Bellingham, WA: SPIE, 1997, ch. 7.

[20] D. O. Caplan, M. L. Stevens, J. J. Carney, and R. J. Murphy, "Demonstration of optical DPSK communication with 25 photons/bit receiver sensitivity," presented at the Conf. Lasers Electr.-Opt., Long Beach, CA, May 21–26, 2006, Paper CFH5.

[21] J. H. Sinsky, A. Adamiecki, A. Gnauck, C. A. Burrus, Jr., J. Leuthold, O. Wohlgemuth, S. Chandrasekhar, and A. Umbach, "RZ-DPSK transmission using a 42.7-Gb/s integrated balanced optical front end with record sensitivity," *J. Lightw. Technol.*, vol. 22, no. 1, pp. 180–185, Jan. 2004.

[22] N. W. Spellmeyer, J. C. Gottschalk, D. O. Caplan, and M. L. Stevens, "High-sensitivity 40-Gb/s RZ-DPSK with forward error correction," *IEEE Photon. Technol. Lett.*, vol. 16, no. 6, pp. 1579–1581, Jun. 2004.

[23] E. A. Swanson, J. C. Livas, and R. S. Bondurant, "High sensitivity optically preamplified direct detection DPSK receiver with active delay-line stabilization," *IEEE Photon. Technol. Lett.*, vol. 6, no. 2, pp. 263–265, Feb. 1994.

[24] D. O. Caplan, M. L. Stevens, and J. J. Carney, "High-sensitivity multichannel single-interferometer DPSK receiver," *Opt. Exp.*, vol. 14, no. 23, pp. 10984–10989, Nov. 13, 2006.

[25] A. Belmonte, A. Comerón, J. A. Rubio, J. Bará, and E. Fernández, "Atmospheric-turbulence-induced power-fade statistics for a multiaperture optical receiver," *Appl. Opt.*, vol. 36, no. 33, pp. 8632–8638, Nov. 20, 1997.

[26] A. R. Weeks, J. Xu, R. R. Phillips, L. C. Andrews, C. M. Stickley, G. Sellar, J. S. Stryjewski, and J. E. Harvey, "Experimental verification and theory for an eight-element multiple-aperture equal-gain coherent laser receiver for laser communications," *Appl. Opt.*, vol. 37, no. 21, pp. 4782–4788, Jul. 20, 1998.

[27] L. C. Andrews, "Free space optical communication link and atmospheric effects: single aperture and arrays," *Proc. SPIE*, vol. 5338, pp. 265–275, 2004.

[28] F. G. Walther, J. D. Moores, R. J. Murphy, S. Michael, and G. N. Nowak, "A process for free-space laser communications system design," *Proc. SPIE*, vol. 7464, pp. 74640V-1–74640V-9, 2009.

[29] J. D. Moores, G. G. Walther, J. A. Greco, S. Michael, W. E. Wilcox, Jr., A. M. Volpicelli, R. J. Magliocco, and S. R. Henion, "Architecture overview and data summary of a 5.4 km free-space laser communications experiment," *Proc. SPIE*, vol. 7464, pp. 746404-1–746404-9, 2009.

[30] T. Williams, R. J. Murphy, F. Walther, A. Volpicelli, B. Willcox, and D. Crucioli, "A free-space optical terminal for fading channels," *Proc. SPIE*, vol. 7464, pp. 74640W-1–74640W-7, 2009.

[31] H. Kim and P. J. Winzer, "Robustness to laser frequency offset in direct-detection DPSK and DQPSK systems," *J. Lightw. Technol.*, vol. 21, no. 9, pp. 1887–1891, Sep. 2003.

[32] A. K. Dutta, N. K. Dutta, and M. Fujiwara, *WDM Technologies: Active Optical Components*. San Diego, CA: Academic Press, 2002, ch. 4.

[33] ILX Lightwave Laser Diode Temperature Controller Selection Guide. [Online]. Available: http://www.ilxlightwave.com/selection-guide/laser-diode-temperature-controllers-selection-guide.html

[34] T. G. Ulmer, S. R. Henion, F. G. Walther, and P. A. Schulz, "Differential phase-shift keying in multi-wavelength spatial diversity links," presented at the Appl. Lasers Sens. Free Space Commun. OSA Top. Meeting, San Diego, CA, Jan. 31–Feb. 4, 2010.

[35] L. C. Andrews and R. L. Phillips, *Laser Beam Propagation through Random Media*. Bellingham, WA: SPIE, 1998, ch. 9.

Todd G. Ulmer (M'92) was born in Pennsylvania in 1970. He received the B.S. degree in physics magna cum laude from Furman University, Greenville, SC, in 1993, the B.E.E. degree with highest honors from the Georgia Institute of Technology, Atlanta, in 1994, and the M.S. and Ph.D. degrees in electrical engineering from the Georgia Institute of Technology in 1996 and 2000, respectively. His dissertation research involved an integrated-optical serial-to-parallel converter for optical time-division demultiplexing that utilized microcavity-enhanced surface-emitted second-harmonic generation in semiconductor waveguides.

In 2001, he joined the Optical Communications Technology group at MIT Lincoln Laboratory, Lexington, where he investigated wideband analog optical links, fiber Bragg gratings, automatic polarization controllers, and high-power optical amplifiers. He is currently a Staff Member with the Advanced Lasercom Systems and Operations Group, MIT Lincoln Laboratory, where he is engaged in research on free-space optical communications. His research interests include integrated optical devices and nonlinear optics in semiconductors and optical fiber.

Dr. Ulmer is a member of the IEEE Photonics Society, the Optical Society of America, and Phi Beta Kappa.

Scott R. Henion was born in Cleveland, OH, in 1961. He received the B.S. degree in physics from the State University of New York, Brockport, in 1983, and the M.S. degree in physics from the University of Massachusetts, Lowell, in 1988.

He joined MIT Lincoln Laboratory, Lexington, in 1988, where he was engaged in research on solid-state lasers, analog fiber-optic communication, and microwave photonic signal processing. From 1999 to 2003, he was with PhotonEx Corporation, Maynard, MA, where he developed fiber-optic communication systems. In 2003, he returned to MIT Lincoln Laboratory, where he is currently an Associate Staff Member in the Advanced Lasercom Systems and Operations Group, developing high-speed fiber-optic transceivers.

Frederick G. Walther (M'72) received the B.A. degree in physics from Yale University, New Haven, CT, in 1967 and the Ph.D. degree in physics from the Massachusetts Institute of Technology, Cambridge, in 1972.

He served in the United States Air Force at the Air Force Cambridge Research Laboratory before joining MIT Lincoln Laboratory, Lexington, MA, as a Technical Staff Member in 1973. He has been a member of the Communications Division at Lincoln for 36 years, developing optical communication systems for the past 28 years, and is currently Assistant Group Leader of the Advanced Lasercom Systems and Operations Group. His research has addressed various system issues in lasercom, particularly pointing and tracking systems, and currently centers on the challenges of high-data-rate lasercom through the turbulent lower atmosphere.

Dr. Walther is a member of IEEE and the American Physical Society.

Peter A. Schulz (M'91) was born in Boston, MA, in 1954. He received the B.S. degree from the Massachusetts Institute of Technology, Cambridge, and the Ph.D. degree from the University of California, Berkeley, both in physics.

While with the Joint Institute for Laboratory Astrophysics at the University of Colorado, he studied negative ions using threshold photodetachment spectroscopy. After joining the faculty of the Georgia Institute of Technology in 1982, he studied photodissociation and molecular beam kinetics using high-resolution vacuum ultraviolet and microwave spectroscopies. As a 1985 summer Fellow at Oak Ridge National Laboratory, he studied electron-impact ionization of multiply charged ions and electron-impact dissociation of H_3O+. Since 1986 he has been at MIT Lincoln Laboratory, where he has developed $Ti{:}Al_2 0_3$ lasers, frequency-modulated Nd:YAG lasers, and dispersion compensated Faraday isolators. More recently he has worked on optical networking and fiber-optic communication transceivers. He is currently a Staff Member at Lincoln, working at the Reagan Test Site on the Kwajalein Atoll. His research interests include laser dynamics, novel lasers, electro-optics, and optical communication.

Dr. Schulz is a member of the Optical Society of America.